Chapter 3
Dissipation, Noise and Adaptive Systems

Most dynamical systems are not isolated, but interacting with an embedding environment that may add stochastic components to the evolution equations. The internal dynamics slows down when energy is dissipated to the outside world, approaching attracting states which may be regular, such as fixpoints or limit cycle, or irregular, such as chaotic attractors. Adaptive systems alternate between phases of energy dissipation and uptake, until a balance between these two opposing processes is achieved.

In this chapter an introduction to adaptive, dissipative and stochastic systems will be given together with important examples from the realm of noise controlled dynamics, like diffusion, random walks and stochastic escape and resonance. We will discuss to which extent chaos, a regular guest of adaptive systems, may remain predictable.

3.1 Chaos in Dissipative Systems

The time evolution of deterministic systems can be computed exactly, at least as matter of principle, once the initial conditions are known.[1] We now turn to "stochastic systems", i.e. dynamical systems that are influenced by noise and fluctuations. On a mean level, the impact of noise shows up as "dissipation".

3.1.1 Phase Space Contraction and Expansion

Friction and Dissipation Friction plays an important role in real-world systems, causing energy to be dissipated to the environment.

[1] For references, Chap. **??**, "**??**" is devoted to determinstic dynamics.

Energy is conserved when the contributions from all constituent parts of the overall system are taken into account. Friction just stands for a transfer process of energy; when energy is transferred from a system we observe, like a car on a motorway with the engine turned off, to a system not under observation, such as the surrounding air. In this case the combined kinetic energy of the car and the thermal energy of the air body remains constant; the air heats up a little bit while the car slows down.

Mathematical Pendulum As an example we consider the damped mathematical pendulum,

$$\ddot{\phi} + \gamma\dot{\phi} + \omega_0^2 \sin\phi = 0\,, \tag{3.1}$$

which describes a pendulum with a rigid bar, capable of turning over completely, with ϕ corresponding to the angle between the bar and the vertical.

The mathematical pendulum reduces to the damped harmonic oscillator for small $\phi \approx \sin\phi$, which is damped/critical/overdamped for $\gamma < 2\omega_0$, $\gamma = 2\omega_0$ and $\gamma > 2\omega_0$. In the absence of damping, $\gamma = 0$, the energy

$$E = \frac{\dot{\phi}^2}{2} - \omega_0^2 \cos\phi \tag{3.2}$$

is conserved,

$$\frac{d}{dt}E = \dot{\phi}\,\ddot{\phi} + \omega_0^2\dot{\phi}\sin\phi = \dot{\phi}\left(\ddot{\phi} + \omega_0^2\sin\phi\right) = -\gamma\dot{\phi}^2\,,$$

when using (3.1).

Normal Coordinates Transforming the damped mathematical pendulum (3.1) to a set of coupled first-order differential equations via $x = \phi$ and $\dot{\phi} = y$ one gets

$$\begin{aligned} \dot{x} &= y \\ \dot{y} &= -\gamma y - \omega_0^2 \sin x\,. \end{aligned} \tag{3.3}$$

The phase space for $\mathbf{x} = (x, y)$ $\boldsymbol{R}^2$. For all $\gamma > 0$ the motion approaches for $t \to \infty$ one of the equivalent global fixpoints $(2\pi n, 0)$, where $n \in \boldsymbol{Z}$.

Phase Space Contraction By definition, phase space contracts close to an attractor. For a three-dimensional phase space, $\mathbf{x} = (x, y, z)$, the quantity

$$\begin{aligned} \Delta V(t) &= \Delta x(t)\Delta y(t)\Delta z(t) \\ &= (x(t) - x'(t))\,(y(t) - y'(t))\,(z(t) - z'(t)) \end{aligned}$$

corresponds to a small volume in phase space when $|\mathbf{x} - \mathbf{x}'|$ is small. Its time evolution is given by

$$\frac{d}{dt}\Delta V = \Delta\dot{x}\Delta y\Delta z + \Delta x\Delta\dot{y}\Delta z + \Delta x\Delta y\Delta\dot{z}\,,$$

or

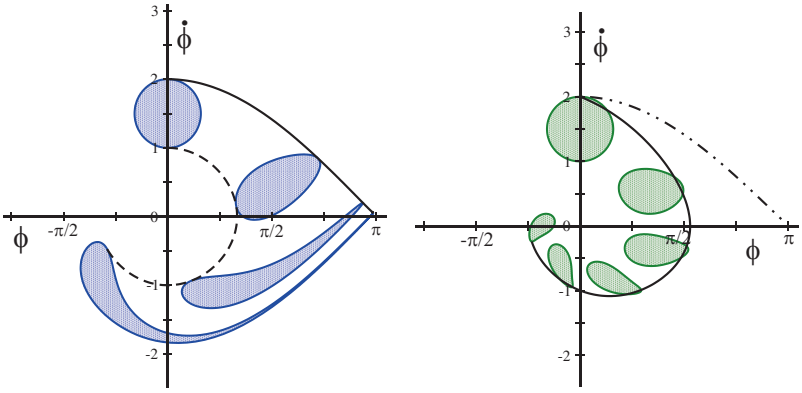

Fig. 3.1 Simulation of the mathematical pendulum $\ddot{\phi} = -\sin(\phi) - \gamma\dot{\phi}$, illustrating the evolution of the phase space volume for consecutive times (shaded regions), starting with $t = 0$ (top). **Left:** The dissipationless case $\gamma = 0$. The energy, see (3.2), is conserved as well as the phase space volume (Liouville's theorem). Shown are trajectories for $E = 1$ and $E = -0.5$ (solid/dashed line). **Right:** For $\gamma = 0.4$. Note the consecutive contraction of the phase space volume.

$$\frac{\Delta\dot{V}}{\Delta x \Delta y \Delta z} = \frac{\Delta\dot{x}}{\Delta x} + \frac{\Delta\dot{y}}{\Delta y} + \frac{\Delta\dot{z}}{\Delta z} = \boldsymbol{\nabla} \cdot \dot{\mathbf{x}}\,, \tag{3.4}$$

with the right-hand side corresponding to the trace of the Jacobian.

In Fig. 3.1 the time evolution of a phase space volume is illustrated for the case of the mathematical pendulum. Volumes of the phase space remain connected under the effect of the time evolution, undergoing however at times substantial deformations.

Dissipative and Conserving Systems A dynamical system is dissipative, if its phase space volume contracts continuously, viz when $\boldsymbol{\nabla} \cdot \dot{\mathbf{x}} < 0$ for all $\mathbf{x}(t)$. The system is said to be conserving if the phase space volume is a constant of motion, viz if $\boldsymbol{\nabla} \cdot \dot{\mathbf{x}} \equiv 0$.

Mechanical systems, i.e. systems described by Hamiltonian mechanics, are conserving in above sense. One denotes this result from classical mechanics as "Liouville's theorem".

Depending on the energy, mechanical systems may have bounded or non-bounded orbits. Planets run through bounded orbits around the sun, to give an example, with certain comets leaving the solar system for ever on unbounded trajectories. One can easily deduce from Liouville's theorem, i.e. from phase space conservation, that bounded orbits are "ergodic". They come arbitrarily close to all points in phase space having the identical conserved energy.

Global Dissipation Dissipation may occur everywhere in phase space, or only locally. The first holds for the damped mathematical pendulum (3.3),

$$\frac{\partial \dot{x}}{\partial x} = 0, \qquad \frac{\partial \dot{y}}{\partial y} = \frac{\partial[-\gamma y - \omega_0^2 \sin x]}{\partial y} = -\gamma\,,$$

which implies

$$\boldsymbol{\nabla} \cdot \dot{\mathbf{x}} = -\gamma < 0\,.$$

The damped harmonic oscillator is consequently globally dissipative. The basin of attraction of the fixpoint $(0, 0)$ covers the full phase space (modulo 2π). Selected trajectories are illustrated in Fig. 3.1 together with phase space contraction.

Local Dissipation For the non-linear rotator defined by (**??**),

$$\dot{r} = (\Gamma - r^2)\, r, \qquad \dot{\varphi} = \omega\,, \tag{3.5}$$

we have

$$\frac{\partial \dot{r}}{\partial r} + \frac{\partial \dot{\varphi}}{\partial \varphi} = \Gamma - 3r^2 = \begin{cases} < 0 \text{ for } \Gamma < 0 \\ < 0 \text{ for } \Gamma > 0 \;\text{ and }\; r > r_c/\sqrt{3} \\ > 0 \text{ for } \Gamma > 0 \;\text{ and }\; 0 < r < r_c/\sqrt{3} \end{cases}, \tag{3.6}$$

where $r_c = \sqrt{\Gamma}$ is the radius of the limit cycle existing when $\Gamma > 0$. The system might either dissipate or take up energy, which is typical behavior of adaptive systems, as we will discuss further in Sect. 3.2.

Phase space contracts globally when $\Gamma < 0$, and locally, close to the limit cycle, when $\Gamma > 0$. In the latter case, when $\Gamma > 0$, phase space expands around the unstable fixpoint $(0, 0)$.

Coordinate Transformation The time development of a small phase space volume, as defined by (3.4), depends on the coordinate system chosen to represent the variables. As an example we reconsider the non-linear rotator (3.5) in terms of the Cartesian coordinates $x = r\cos\varphi$ and $y = r\sin\varphi$.

The respective infinitesimal phase space volumes are related via the Jacobian,

$$dx\, dy = r\, dr\, d\varphi\,,$$

and we find

$$\frac{\dot{\Delta V}}{\Delta V} = \frac{\dot{r}\Delta r\Delta\varphi + r\dot{\Delta} r\Delta\varphi + r\Delta r\dot{\Delta}\varphi}{r\Delta r\Delta\varphi} = \frac{\dot{r}}{r} + \frac{\partial \dot{r}}{\partial r} + \frac{\partial \dot{\varphi}}{\partial \varphi} = 2\Gamma - 4r^2\,.$$

Comparing with (3.6) we see that the amount and even the sign of phase space contraction can depend on the choice of the coordinate system. However, phase space will always contract close to an attractor, regardless of the coordinate system selected. This hold for $(0, 0)$ when $\Gamma < 0$ and for the limit cycle at $r = \sqrt{\Gamma}$ when $\Gamma > 0$.

Divergence of the Flow and Lyapunov Exponents For a dynamical system $\dot{\mathbf{x}} = \mathbf{f}(\mathbf{x})$ the local change in phase space volume is given by the

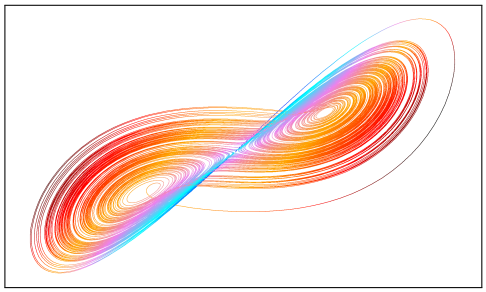

Fig. 3.2 A typical trajectory of the Lorenz system (3.8), for the classical set of parameters, $\sigma = 10$, $b = 8/3$ and $r = 28$. The chaotic orbit loops around the remnants of the two fixpoints (3.9), which are unstable for the selected set of parameters. Color coding with respect to z, projected to the $z = 0$ plane.

divergence of the flow,

$$\frac{\dot{\Delta V}}{\Delta V} = \boldsymbol{\nabla} \cdot \mathbf{f} = \sum_i \frac{\partial f_i}{\partial x_i} = \sum_i \lambda_i \,, \tag{3.7}$$

and hence by the trace of the Jacobian $J_{ij} = \partial f_i / \partial x_j$, as mentioned before. The trace of a matrix corresponds to the sum $\sum_i \lambda_i$ of its eigenvalues λ_i. Phase space hence contracts when the sum of the local Lyapunov exponents is negative.

3.1.2 Strange Attractors and Dissipative Chaos

Lorenz Model A rather natural question regards the possible existence of attractors with irregular behaviors, i.e. which are different from stable fixpoints, periodic or quasi-periodic motion. For this question we examine the Lorenz model

$$\begin{aligned} \dot{x} &= -\sigma(x - y), \\ \dot{y} &= -xz + rx - y, \\ \dot{z} &= xy - bz \,. \end{aligned} \tag{3.8}$$

The classical values are $\sigma = 10$ and $b = 8/3$, with r being the control variable.

Fixpoints of the Lorenz Model A trivial fixpoint is $(0, 0, 0)$. The non-trivial fixpoints are

$$\begin{aligned} 0 &= -\sigma(x - y), & x &= y, \\ 0 &= -xz + rx - y, & z &= r - 1, \\ 0 &= \quad xy - bz, & x^2 &= y^2 = b\,(r - 1)\,. \end{aligned}$$

It is easy to see by linear analysis that the fixpoint $(0, 0, 0)$ is stable for $r < 1$. For $r > 1$ it becomes unstable via a pitchfork bifurcation and two new fixpoints appear,

$$C_{\pm} = \left(\pm\sqrt{b(r-1)}, \pm\sqrt{b(r-1)}, r-1\right) . \tag{3.9}$$

These are stable for $r < r_c = 24.74$ (for $\sigma = 10$ and $b = 8/3$), at which point a subcritical Hopf bifurcation occurs. Generally one has $r_c = \sigma(\sigma + b + 3)/(\sigma - b - 1)$. For $r > r_c$ the behavior becomes more complicated and generally non-periodic.

Strange Attractors One can show, that the Lorenz model has a positive Lyapunov exponent for $r > r_c$. It is chaotic with sensitive dependence on the initial conditions. A typical orbit is illustrated in Fig. 3.2. The Lorenz model is at the same time globally dissipative, since

$$\frac{\partial \dot{x}}{\partial x} + \frac{\partial \dot{y}}{\partial y} + \frac{\partial \dot{z}}{\partial z} = -(\sigma + 1 + b) < 0, \qquad \sigma, b > 0 . \tag{3.10}$$

The consequence is that the attractor of the Lorenz system cannot be a smooth surface. Close to the attractor phase space contracts. At the same time two nearby orbits are repelled due to the positive Lyapunov exponents. One finds a self-similar structure for the Lorenz attractor with a fractal dimension 2.06 ± 0.01, as defined further below. Such a structure is called a "strange attractor".

Dissipative Chaos and Strange Attractors Strange attractors can only occur in dynamical system of dimension three and higher, in one dimension fixpoints are the only possible attracting states and one needs at least two dimensions for limit cycles.

The Lorenz model has an important historical relevance for the development of chaos theory It is considered a paradigmatic model, since chaos in dissipative and deterministic dynamical systems is closely related to the emergence of strange attractors. Chaos may arise in one dimensional maps, as we see in Sect. **??**, but continuous-time dynamical systems need to be at least three dimensional in order to show chaotic behavior.

Hyperchaos An attractor is chaotic when at least a single Lyapunov exponent is positive. As a function of the position on the attracting manifold, local Lypunov exponets may vary substantially, which implies that the occurance of chaos is determined by the sign of the maximal Lypunov, compare the corresponding definition (**??**) for maps. Several Lypunov exponents may become positive for systems with larger numbers of dynamical variables, such as dynamical networks. One speaks of "hyperchaos" when this happens.

Fractals Strange attractors often show a high degree of self-similarity, being fractal. Fractals can be defined on an abstract level by recurrent geometric rules, prominent examples are the Cantor set, the Sierpinski triangle and the Sierpinski carpet illustrated in Fig. 3.3. Strange attractors are normally "multi fractal", i.e. fractals with non-uniform self similarity.

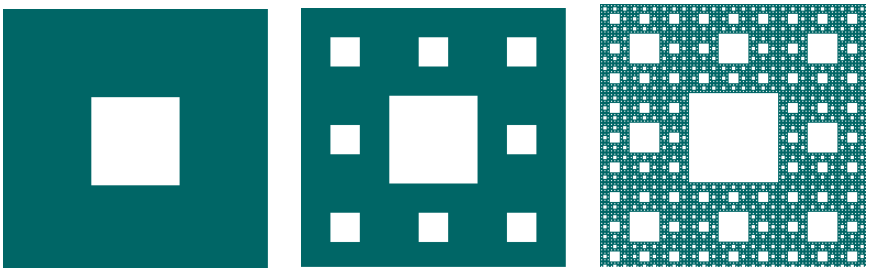

Fig. 3.3 The Sierpinski carpet and its iterative construction.

Hausdorff Dimension An important notion in the theory of fractals is the "Hausdorff dimension". We consider a geometric structure defined by a set of points in d dimensions and the number $N(l)$ of d-dimensional spheres of diameter l needed to cover this set. If $N(l)$ scales like

$$N(l) \;\propto\; l^{-D_H}\,, \qquad \text{for} \qquad l \;\to\; 0\,, \tag{3.11}$$

then D_H is called the Hausdorff dimension of the set. Alternatively we can rewrite (3.11) as

$$\frac{N(l)}{N(l')} = \left(\frac{l}{l'}\right)^{-D_H}\,, \qquad D_H = -\frac{\log[N(l)/N(l')]}{\log[l/l']}\,, \tag{3.12}$$

which is useful for self-similar structures (fractals).

The d-dimensional spheres necessary to cover a given geometrical structure will generally overlap. The overlap does not affect the value of the fractal dimension as long as the degree of overlap does not change qualitatively with decreasing diameter l.

Hausdorff Dimension of the Sierpinski Carpet For the Sierpinski carpet we increase the number of points $N(l)$ by a factor of eight when we decrease the length scale l by a factor of three,

$$D_H \;\to\; -\frac{\log[8/1]}{\log[1/3]} = \frac{\log 8}{\log 3} \approx 1.8928\,.$$

See Fig. 3.4 for an illustration.

3.1.3 Partially Predictable Chaos

The strange attractor of the Lorenz model has the form of a 'butterfly', but otherwise seemingly no further internal structure. Orbits exponentially diverge close to the attractor, remaining however bounded by its overall size.

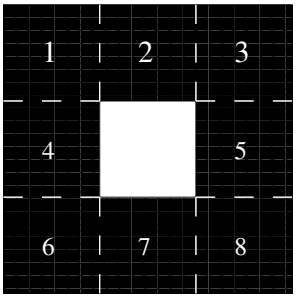

Fig. 3.4 The fundamental unit of the Sierpinski carpet, compare Fig. 3.3. It contains eight squares which can be covered by discs of appropriate diameter.

The only feature remaining predictable is that orbits will not diverge indefinitely. The sistuation is more complex for most real-world chaotic systems.

As an example of a real-world system with substantial chaotic components we may take weather forecasting. When a hurricane approaches a coastline, one may not be able to predict the location of landfall precisely, nor the strength of the hurricane at that point. Nobody will doubt however, that a full-blown hurricane is approaching. Certain features can remain predictable even in otherwise chaotic systems. This is the notion of "partially predictable chaos", which we will examine in the following.

For a precise definition of partially predictable chaos one needs an observational tool allowing to determine the presence of chaos directly from the properties of typical orbits, without resorting to the evaluation of Lyapunov exponents. This tool, a "0-1 test for chaos", is developed first.

Initially Close Orbits For a given dynamical system we examine the long-term fate of two initially close orbits, $\mathbf{x} = \mathbf{x}(t)$ and $\mathbf{x}' = \mathbf{x}'(t)$, with

$$\Delta X_0 = ||\mathbf{x} - \mathbf{x}'||_{t=0}$$

being small. We are interested in the average long-term inter-orbit distance,

$$\Delta X_\infty = \left\langle ||\mathbf{x} - \mathbf{x}'|| \right\rangle_{t>T}, \tag{3.13}$$

which is defined as the average distance between $\mathbf{x}$ and $\mathbf{x}'$ for times $t > T$, where T is larger than the time scales of the defining dynamical system.

0-1 Test for Chaos In Fig. 3.5 the evolution for two initial close orbits is illustrated for the case that both orbits approach the same attractor, which may be a fixpoint, limit cycle, or a chaotic attractor.

- Fixpoint
  One has $\Delta X_\infty \to 0$ independently of ΔX_0.
- Limit Cycle
  When ΔX_0 is small, substantially smaller than the size of the attracting limit cycle, one observes $\Delta X_\infty \propto \Delta X_0$. The two orbits will follow each

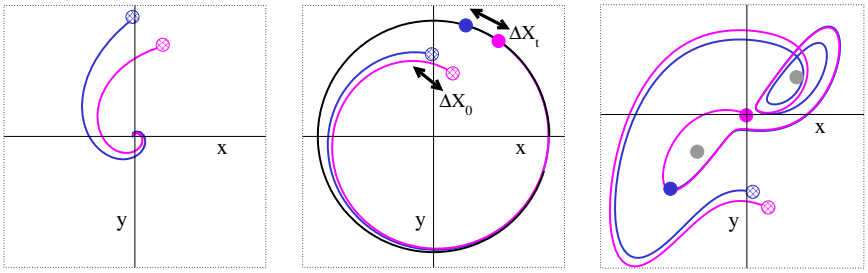

Fig. 3.5 The evolution of two initially close trajectories (blue/magenta lines). The respective initial states (shaded circles) are evolved for the identical period t (filled circles). Shown are orbits for the non-linear rotator (3.5), for $\Gamma < 0$ (left panel) and $\Gamma > 0$ (middle panel), which converge respectively to a stable focus and limit cycle (black ring). For the Lorenz model (right panel), trajectories diverge on the attractor, with one orbit circling one of the unstable fixpoints (grey circles) an additional time. Parameters as in Fig. 3.2.

other indefinitely after having entered the limit cycles at slightly different points, with the average distance ΔX_∞ scaling linearly with ΔX_0

– Chaotic Attractor
Orbits fully decorrelate on the attractor, with ΔX_∞ approaching the average two-point distance irrespectively of ΔX_0.

Above rules constitute a "0-1 test" for chaos. Operationally, one integrates the system in question for pairs of initially close orbits. The resulting average final distance ΔX_∞ is plotted relative to its initial value. The attracting state is a limit cycle if ΔX_∞ scales with ΔX_0, otherwise a fixpoint or a chaotic attractor.

Partially Predictable Chaos Decorrelation is characterized by a single time scale for classical chaotic attractors, such as the butterfly attractor illustrated in Fig. 3.2. The incurring loss of information is captured by the time development of the inter-orbit distance, ΔX_t, as illustrated in Fig. 3.6. Chaos remains however partially predictable when decorrelation is limited for prolonged periods. In this case, when two orbits retain a certain finite distance, one can evaluate their relative development with an accuracy given by the respective ΔX_t. One can still predict what is going to happen for extended time spans, albeit with a finite accuracy. The whole process is shown in Fig. 3.6.

As a function of the control parameter r, a variety of attracting states appear in the Lorenz model. For $r = 28$ the classical butterfly attractor is observed, see Fig. 3.2. For larger values of r, windows with period-doubling limit cycles appear. Interestingly, for certain values of r, like $r = 180.78$, a distinct type of chaotic attractors is observed, in the form of chaotic braids. Topologically, these braids correspond to chaotically broadened limit cycles. Decorrelation slows down by orders of magnitude once ΔX_t becomes comparable to the width of the braids. The subsequent diffusive decorrelation along

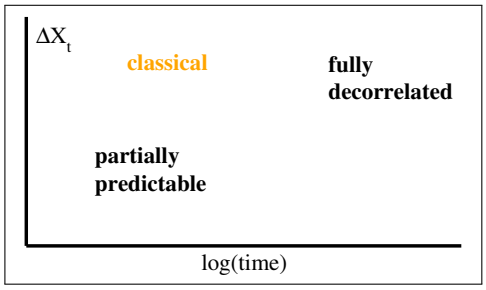

Fig. 3.6 Chaotic dynamics is partially predictable (black curve) when the distance ΔX_t of two initially close orbits remains at a temporary plateau after the starting divergence. The fully decorrelated final state is reached only after a substantial delay. Information is lost within a single process for classical chaos (orange curve).

the former limit cycle is very slow. This is a typical example of partially predictable chaos.

3.2 Adaptive Systems

In general, complex systems are neither fully conserving nor fully dissipative. Adaptive systems will have phases where they take up energy and periods where they give energy back to the environment. An example is the non-linear rotator defined in (3.5), see also (3.6).

One affiliates with the term "adaptive system" often to the notion of complexity and adaption. Strictly speaking, any dynamical system is adaptive if $\boldsymbol{\nabla} \cdot \dot{\mathbf{x}}$ may take both positive and negative values. In practice, however, it is usual to reserve the term adaptive system to dynamical systems showing a certain complexity, such as emerging behavior.

Van der Pol Oscillator Circuits or mechanisms built for the purpose of controlling an engine or machine are intrinsically adaptive. An example is the Van der Pol oscillator,

$$\ddot{x} - \epsilon(1-x^2)\dot{x} + x = 0, \qquad \begin{aligned} \dot{x} &= y \\ \dot{y} &= \epsilon(1-x^2)y - x \end{aligned} \tag{3.14}$$

where $\epsilon > 0$ and where we did use the phase space variables $\mathbf{x} = (x, y)$. The evolution of the phase space volume is

$$\nabla \cdot \dot{\mathbf{x}} = \epsilon\,(1-x^2)\,.$$

The oscillator takes up/dissipates energy for $x^2 < 1$ and $x^2 > 1$, respectively. A simple mechanical example for a system with similar properties is illustrated in Fig. 3.7

Secular Perturbation Theory We consider a perturbation expansion in ϵ. For $\epsilon = 0$, the solution of (3.14) describes harmonic oscillations,

$$x_0(t) = a\,\mathrm{e}^{i(\omega_0 t+\phi)} + c.c., \qquad \omega_0 = 1\,. \tag{3.15}$$

Amplitude a and phase ϕ are arbitrary, as usual for harmonic oscillators. The perturbation $\epsilon(1-x^2)\dot{x}$ may change both the amplitude and the unperturbed frequency $\omega_0 = 1$ by an amount $\propto \epsilon$. In order to account for this "secular perturbation" we make the ansatz

$$x(t) = \left[A(T)\mathrm{e}^{it} + A^*(T)\mathrm{e}^{-it}\right] + \epsilon x_1, \qquad A(T) = A(\epsilon t)\,, \tag{3.16}$$

which differs from the usual expansion $x(t) \to x_0(t)+\epsilon x'(t)$ of the full solution $x(t)$ of a dynamical system with respect to a small parameter ϵ. The yet to be determined time-dependent complex prefactor A allows for an adaption of the original frequency. The ansatz $A = A(\epsilon t)$ ensures that the prefactor is constant when $\epsilon \to 0$.

Expansion The goal is to expand the Van der Pol oscillator together with (3.16) with respect to the perturbation[2] We start be evaluating several expressions involing $x(t)$ up to order $O(\epsilon^1)$, namely

$$\begin{aligned}
x^2 &\approx A^2\mathrm{e}^{2it} + 2|A|^2 + (A^*)^2\mathrm{e}^{-2it} + 2\epsilon x_1\left[A\mathrm{e}^{it} + A\mathrm{e}^{-it}\right] \\
\epsilon(1-x^2) &\approx \epsilon(1-2|A|^2) - \epsilon\left[A^2\mathrm{e}^{2it} + (A^*)^2\mathrm{e}^{-2it}\right], \\
\dot{x} &\approx \left[(\epsilon A_T + iA)\,\mathrm{e}^{it} + c.c.\right] + \epsilon\,\dot{x}_1, \qquad A_T = \frac{\partial A(T)}{\partial T} \\
\epsilon(1-x^2)\dot{x} &= \epsilon(1-2|A|^2)\left[iA\mathrm{e}^{it} - iA^*\mathrm{e}^{-it}\right] \\
&\quad - \epsilon\left[A^2\mathrm{e}^{2it} + (A^*)^2\mathrm{e}^{-2it}\right]\left[iA\mathrm{e}^{it} - iA^*\mathrm{e}^{-it}\right]
\end{aligned}$$

and

$$\begin{aligned}
\ddot{x} &= \left[\left(\epsilon^2 A_{TT} + 2i\epsilon A_T - A\right)\mathrm{e}^{it} + c.c.\right] + \epsilon\,\ddot{x}_1 \\
&\approx \left[(2i\epsilon A_T - A)\,\mathrm{e}^{it} + c.c.\right] + \epsilon\ddot{x}_1\,.
\end{aligned}$$

Substituting these expressions into (3.14), we obtain

$$\ddot{x}_1 + x_1 = \left(-2iA_T + iA - i|A|^2A\right)\mathrm{e}^{it} - iA^3\mathrm{e}^{3it} + c.c.\,, \tag{3.17}$$

to order $O(\epsilon^1)$.

Solvability Condition The time dependencies

$$\sim \mathrm{e}^{it} \qquad \text{and} \qquad \sim \mathrm{e}^{3it}$$

of the two terms on the right-hand side of (3.17) are proportional to the unperturbed frequency $\omega_0 = 1$ and to $3\omega_0$, respectively.

[2] The following derivations are informative, but somewhat advanced. In case, the reader may skip directly to the result, Eq. (3.18).

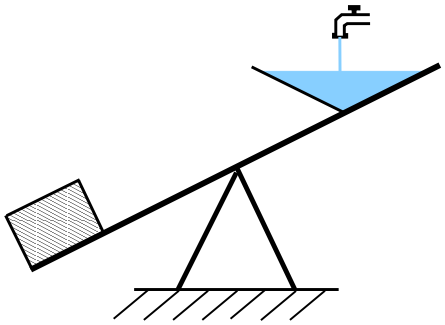

Fig. 3.7 The seesaw with a water container at one end; an example of an oscillator that takes up and disperses energy periodically.

Eq. (3.17) is identical to that of a driven harmonic oscillator.[3] The term $\sim \mathrm{e}^{it}$ is therefore exactly at resonance and would induce a diverging response $x_1 \to \infty$, in contradiction to the perturbative assumption made by ansatz (3.16). Its prefactor must therefore vanish,

$$A_T = \frac{\partial A}{\partial T} = \frac{1}{2}\left(1 - |A|^2\right) A, \qquad \frac{\partial A}{\partial t} = \frac{\epsilon}{2}\left(1 - |A|^2\right) A\,, \tag{3.18}$$

where we used $T = \epsilon t$. The solvability condition (3.18) can be written as

$$\dot{a}\,\mathrm{e}^{i\phi} + i\dot{\phi}\,a\,\mathrm{e}^{i\phi} = \frac{\epsilon}{2}\left(1 - a^2\right) a\,\mathrm{e}^{i\phi}\,,$$

in phase-magnitude representation $A(t) = a(t)\mathrm{e}^{i\phi(t)}$, or

$$\dot{a} = \epsilon\left(1 - a^2\right) a/2, \qquad \dot{\phi} \sim O(\epsilon^2)\,. \tag{3.19}$$

The system takes up energy for $a < 1$ and the amplitude a increases till the saturation limit $a \to 1$, the conserving point. For $a > 1$ the system dissipates energy to the environment and the amplitude a decreases, approaching unity for $t \to \infty$, just as we discussed in connection with (3.5).

In the limit $\epsilon \to 0$ the long-term solution of the Van der Pol oscillator is $x(t) \approx 2\,a\cos(t)$, compare (3.16) and (3.19), which constitutes an amplitude-regulated oscillation. This behavior, compare Fig. 3.8, is relevant for technical control tasks.

Liénard Variables For large ϵ it is convenient to define with

$$\epsilon\,\frac{\mathrm{d}}{\mathrm{d}t}Y(t) = -x(t) = \ddot{x}(t) - \epsilon\left(1 - x^2(t)\right)\dot{x}(t) \tag{3.20}$$

[3] The harmonic oscillator is resonant only when the frequency of the perturbation matches the internal frequency. Non-harmonic oscillators may however unstable against rational frequency ratios, as discussed in Sect. **??** of Chap. **??**, "**??**" in the context of the KAM theorem, with regard to the gaps in the Saturn rings.

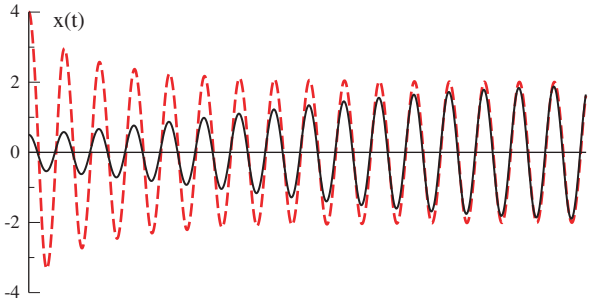

Fig. 3.8 Two solutions of the Van der Pol oscillator (3.14), for small ϵ and two different initial conditions. Note the self-generated amplitude stabilization.

the Liénard variable $Y(t)$, where the second equality is just the definition of the Van der Pol oscillator, see (3.14). With the $X(t) \equiv x(t)$ we rewrite (3.20) as

$$\epsilon \dot{Y} = \ddot{X} - \epsilon \left(1 - X^2\right) \dot{X}, \qquad X(t) = x(t)\,,$$

which we integrate with respect to t,

$$\epsilon Y = \dot{X} - \epsilon \left(X - \frac{X^3}{3} \right) ,$$

where we did set the integration constant to zero. Together with (3.20) we obtain

$$\begin{aligned} \dot{X} &= c \Big(Y - f(X) \Big), \qquad f(X) = X^3/3 - X, \\ \dot{Y} &= -X/c\,, \end{aligned} \tag{3.21}$$

with $c \equiv \epsilon$, as we are now interested in the case $c \gg 1$.

Relaxation Oscillations For a large driving c, we can discuss the solution of the Van der Pol oscillator (3.21) graphically, as illustrated in Fig. 3.9. Of relevance is the flow $(\dot{X}, \dot{Y})$ in phase space (X, Y). For $c \gg 1$ there is a separation of time scales,

$$(\dot{X}, \dot{Y}) \;\sim\; (c, 1/c), \qquad \dot{X} \gg \dot{Y}\,,$$

which leads to the following dynamical behavior:

– Starting at a general $(X(t_0), Y(t_0))$ the orbit develops very fast $\sim c$ and nearly horizontally until it hits the "isocline"[4]

$$\dot{X} = 0, \qquad Y = f(X) = -X + X^3/3\,. \tag{3.22}$$

[4] The term isocline stands for "equal slope" in ancient Greek.

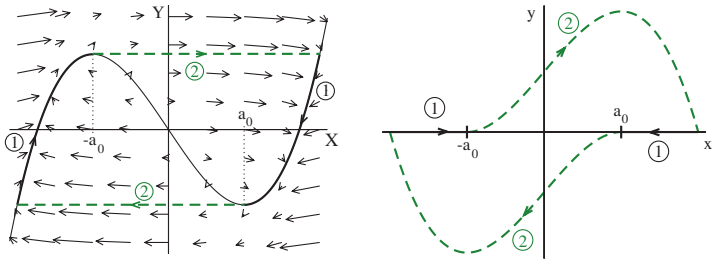

Fig. 3.9 Van der Pol oscillator for a large driving $c \equiv \epsilon$. **Left:** Relaxation oscillations with respect to the Liénard variables (3.21). Indicated is the flow $(\dot{X}, \dot{Y})$ (arrows), for $c = 3$, see (3.21). Also shown is the $\dot{X} = 0$ isocline $Y = -X + X^3/3$ (solid line) and the limit cycle, which includes a non-constant part (dashed line) and a section of the isocline. **Right:** The limit cycle in terms of the original variables $(x, y) = (x, \dot{x}) = (x, v)$. Note that $X(t) = x(t)$.

- Once the orbit is close to the $\dot{X} = 0$ isocline $Y = -X + X^3/3$ the motion slows down, proceeding with a velocity $\sim 1/c$ close-to (but not exactly on) the isocline (3.22).
- Once the slow motion reaches one of the two local extrema $X = \pm a_0 = \pm 1$ of the isocline, it cannot follow the isocline any more and makes a rapid transition towards the other branch of the $\dot{X} = 0$ isocline, with $Y \approx$ const. Note, that trajectories may cross the isocline vertically, which implies that $\dot{Y}|_{X=\pm 1} = \mp 1/c$ is small but finite right at the extrema.

The orbit therefore relaxes rapidly towards a limiting oscillatory trajectory, illustrated in Fig. 3.9, with the time needed to perform a whole oscillation depending on the relaxation constant c; therefore the term "relaxation oscillation". Relaxation oscillators represent an important class of cyclic attractors, allowing to model systems going through several distinct and well characterized phases during the course of one cycle.[5]

3.2.1 Conserving Adaptive Systems

Per definition, conserving dynamical systems conserves the volume of phase space enclosed by a set of trajectories, as illustrated in Fig. 3.1. In contrast, phase space expands and contracts along a given orbit when the system is adaptive, as we discussed for the case of the Van der Pol oscillator, as defined by (3.14), and for the Taken-Bogdanov system.[6] Adaptive systems cannot conserve phase space volume, but they may conserve other quantities, like a generalized energy functional.

[5] We will discuss relaxation oscillators further in Sect. **??** of Chap. **??**, "**??**".

[6] See Sect. **??** of Chap. **??**, "**??**"). for an in-depth treament of the Taken-Bogdanov equations.

Energy Conservation in Mechanical Systems Newton's equation

$$\begin{aligned}\dot{\mathbf{x}} &= \mathbf{v}\\ \dot{\mathbf{v}} &= -\boldsymbol{\nabla} V(\mathbf{x})\end{aligned} \qquad E(\mathbf{x},\mathbf{v}) = \frac{\mathbf{v}^2}{2} + V(\mathbf{x}) \tag{3.23}$$

for a mechanical systems with a potential $V(\mathbf{x})$ conserves energy, $E = E(\mathbf{x},\mathbf{v})$,

$$\frac{dE}{dt} = \frac{\partial E}{\partial \mathbf{x}}\dot{\mathbf{x}} + \frac{\partial E}{\partial \mathbf{v}}\dot{\mathbf{v}} = \big(\boldsymbol{\nabla} V + \dot{\mathbf{v}}\big)\mathbf{v} = 0\,.$$

Energy is an instance of a "constant of motion", viz of a conserved quantity.

Lotka–Volterra Model for Rabbits and Foxes Evolution equations for one or more interacting species are termed "Lotka–Volterra" models. A basic example is that of a prey (rabbit) with population density x being hunted by a predator (fox) with population density y,

$$\begin{aligned}\dot{x} &= Ax - Bxy\\ \dot{y} &= -Cy + Dxy\end{aligned}\,. \tag{3.24}$$

The population x of rabbits can grow by themselves but the foxes need to eat rabbits in order to multiply. All constants A, B, C and D, are positive.

Fixpoints The Lotka–Volterra equation has two fixpoints,

$$\mathbf{x}_0^* = (0,0), \qquad \mathbf{x}_1^* = (C/D, A/B)\,. \tag{3.25}$$

with the respective Jacobians,[7]

$$J_0 = \begin{pmatrix} A & 0\\ 0 & -C\end{pmatrix}, \qquad J_1 = \begin{pmatrix} 0 & -BC/D\\ AD/B & 0\end{pmatrix}.$$

The trivial fixpoint $\mathbf{x}_0^*$ is hence a saddle and $\mathbf{x}_1^*$ a neutral focus with purely imaginary Lyapunov exponents $\lambda = \pm i\sqrt{CA}$. The trajectories circling the focus close onto themselves, as illustrated in Fig. 3.10 for $A = B = C = D = 1$.

Phase space Evolution We now consider the evolution of phase space volume, as defined by (3.4),

$$\frac{\partial \dot{x}}{\partial x} + \frac{\partial \dot{v}}{\partial v} = A - By - C + Dx\,. \tag{3.26}$$

The phase space expands/contracts for y smaller/larger than $(A+Dx-C)/B$, the tell sign of an adaptive system.

[7] We recall that the Jacobian is the matrix of all possible partial derivatives, see Sect. **??**, of Chap. **??**, "**??**".

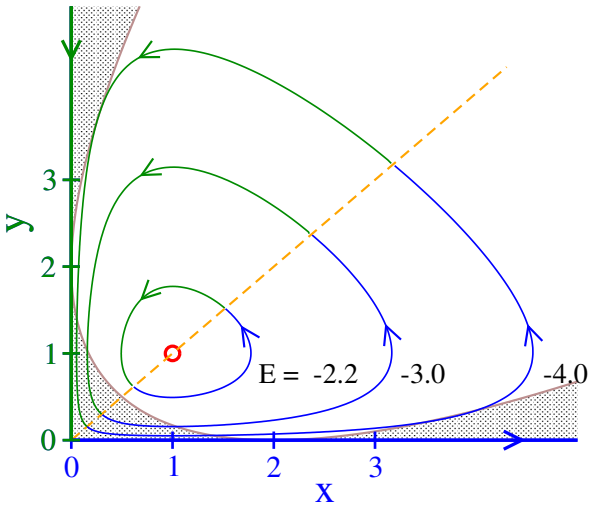

Fig. 3.10 In the space of population densities (x, y), the flow of the fox and rabbit Lotka–Volterra model, see (3.24) and (3.26). The flow expands (contracts) for $x > y$ ($x < y$), as indicated (blue/green orbits). Trajectories coincide with the iso-energy lines of the conserved function E, as defined by (3.27), with $(0, 0)$ being a saddle and $(1, 1)$ a neutral focus (open red circle). Lyapunov exponents are real in the shaded region and complex otherwise.

Constant of Motion The function

$$E(x, y) = A \log(y) + C \log(x) - By - Dx \tag{3.27}$$

on phase space (x, y) is a constant of motion for the Lotka–Volterra model (3.24), since

$$\begin{aligned} \frac{dE}{dt} &= A\dot{y}/y + C\dot{x}/x - B\dot{y} - D\dot{x} \\ &= A(-C + Dx) + C(A - By) - B(-C + Dx)y - D(A - By)x \\ &= 0\,. \end{aligned}$$

The prey-predator system (3.24) does hence dispose of a non-trivial constant of motion. Note that $E(x, y)$ has no biological significance which would be evident per se.

Iso-Energy Manifolds The flow of a d-dimensional dynamical system $\dot{\mathbf{x}} = \mathbf{f}(\mathbf{x})$ disposing of a conserved functional $E(\mathbf{x})$, we call it here a generalized energy, is always restricted to an iso-energy manifold defined by $E(\mathbf{x}) = \text{const}$,

$$\frac{dE}{dt} = \boldsymbol{\nabla} E \cdot \dot{\mathbf{x}} = 0, \qquad \boldsymbol{\nabla} E \perp \dot{\mathbf{x}}\,. \tag{3.28}$$

The flow $\dot{\mathbf{x}}$ is consequently perpendicular to the gradient $\boldsymbol{\nabla} E$ the conserved generalized energy. Orbits are therefore confined to an iso-energy manifold, which is one-dimensional, given that phase space is two-dimensional. Trajectories coincided hence with the iso-energy manifold for the fox and rabbit Lotka–Volterra, as illustrated in Fig. 3.10.

Lyapunov Exponent We evaluate the Jacobian for a generic point (x, y) in phase space,

$$\begin{pmatrix} (1-y) & -x \\ y & (x-1) \end{pmatrix}, \qquad \lambda_\pm = \frac{x-y}{2} \pm \frac{1}{2}\sqrt{(x-y)^2 - 4(x+y-1)}\,,$$

where we did set $A = B = C = D = 1$. The Lyapunov exponents $\lambda_\pm$ are real close to the axes and complex further away, with the separatrix given by

$$(x-y)^2 = 4(x+y-1), \qquad y = x + 2 \pm \sqrt{8x}\,. \tag{3.29}$$

There is no discernible change in the flow dynamics across the separatrix (3.29), which we included in Fig. 3.10, viz when the Lyapunov exponents acquire finite imaginary components.

Invariant Manifolds Fixpoints and limit cycles are examples of invariant subsets of phase space.

INVARIANT MANIFOLD A subset of phase space invariant under the flow for all times $t \in [-\infty, \infty]$ is denoted an invariant manifold.

All trajectories of the fox and rabbit Lotka–Volterra model, apart from the stable and the unstable manifolds of the saddle $(0, 0)$, are closed and constitute hence invariant manifolds.

Fixpoints and limit cycles are invariant manifolds with dimensions zero and one respectively, strange attractors, see Sect. 3.1.1, have generically a fractal dimension.

Closed Invariant Manifolds The evolution of phase space on an invariant manifold (viz inside the manifold) with dimension m is determined by m Lyapunov exponents whenever the manifold has a smooth topology (which is not the case for fractals).

Phase space cannot expand or contract forever for orbits on closed invariant manifolds M, which are finite. This is the case for all trajectories of the fox and rabbit Lotka–Volterra model and manifestly evident for the case $A = B = C = D = 0$ discussed above, for which the real part of the Lyapunov exponent $\lambda_\pm$ is anti-symmetric under the exchange $x \leftrightarrow y$.

Lotka–Volterra system with resource limitation The reproduction of the prey in the original Lotka–Volterra model (3.24) is not limited. In practice, the population density x of the rabbits will be bounded by the carrying capacity $x_{\max}$ of the supporting environment, such that $x < x_{\max}$. The modified model,

$$\dot{x} = Ax\left(1 - \frac{x}{x_{\max}}\right) - Bxy, \qquad \dot{y} = (Dx - C)y\,.$$

has the non-trival fixpoint

$$x^* = \frac{C}{D}, \qquad y^* = \frac{A}{B}\left(1 - \frac{C}{Dx_{\max}}\right), \tag{3.30}$$

which exists for $C < Dx_{\max}$. The population of rabbits is never large enough to support a finite population of foxes in the opposite case, when $C > Dx_{\max}$, which leads to $x \to x_{\max}$ and $y \to 0$. When existing, the steady state defined by (3.30) is stable.

The stability of (3.30) can be shown via a direct evaluation of the respective Jacobian. On a general level one can argue that the resource-limiting factor $1 - x/x_{\max}$ adds a contracting element. It is hence not surprising that the previously neutral fixpoint is stabilized.

3.3 Diffusion and Transport

Deterministic vs. Stochastic Time Evolution So far we discussed concepts of deterministic dynamical systems, governed by sets of coupled differential equations without noise or randomness. At the other extreme are diffusion processes for which the random process dominates the dynamics.

Dissemination of information through social networks is one of many examples where diffusion processes plays a paramount role. The simplest model of diffusion is Brownian motion, which describes the erratic movement of grains suspended in a liquid observed by the botanist Robert Brown as early as 1827. Brownian motion became the prototypical example of a stochastic process with the seminal works of Einstein and Langevin at the beginning of the twentieth century.

3.3.1 Random Walks, Diffusion and Lévy Flights

One-Dimensional Diffusion We start with the random walk of particles along a line, with each particle having an equal probability 1/2 to move left/right at every time step. The probability

$$p_t(x), \qquad x = 0, \pm 1, \pm 2, \ldots\ldots, \qquad t = 0, 1, 2, \ldots$$

to find the particle at time t at position x obeys the master equation

$$p_{t+1}(x) = \frac{p_t(x-1) + p_t(x+1)}{2}. \tag{3.31}$$

Next we take the limit of continuous time and space by generalizing (3.31) to discrete steps Δx and Δt in space and time,

$$\frac{p_{t+\Delta t}(x) - p_t(x)}{\Delta t} = \frac{(\Delta x)^2}{2\Delta t} \frac{p_t(x+\Delta x) + p_t(x-\Delta x) - 2p_t(x)}{(\Delta x)^2}\,, \tag{3.32}$$

where we subtracted on both sides the current distribution $p_t(x)$. Taking the limit $\Delta x, \Delta t \to 0$ in such a way that $(\Delta x)^2/(2\Delta t)$ remains finite, we obtain the diffusion equation

$$\frac{\partial p(x,t)}{\partial t} = D\,\frac{\partial^2 p(x,t)}{\partial x^2}, \qquad D = \frac{(\Delta x)^2}{2\Delta t}\,, \tag{3.33}$$

with D being the diffusion constant. Note that the diffusion equation can be cast into the form of a continuity equation,

$$\dot{p} + \boldsymbol{\nabla}\cdot\mathbf{j} = 0, \qquad \mathbf{j} = -D\,\boldsymbol{\nabla} p\,, \tag{3.34}$$

with the diffusion current $\mathbf{j}$ encoding the diffusive transport of particle from high- to low concentrations.

Solution of the Diffusion Equation The solution $\Phi(x,t)$ of the diffusion equation (3.33) is given by

$$\Phi(x,t) = \frac{1}{\sqrt{4\pi D t}} \exp\left(-\frac{x^2}{4Dt}\right), \qquad \int_{-\infty}^{\infty} \mathrm{d}x\, \Phi(x,t) = 1\,, \tag{3.35}$$

which holds[8] for a localized initial state $\Phi(x, t=0) = \delta(x)$. For the derivation one enters the appropiate derivates,

$$\dot{\Phi} = \frac{-\Phi}{2t} + \frac{x^2\Phi}{4Dt^2}, \qquad \Phi' = \frac{-x\Phi}{2Dt}, \qquad \Phi'' = \frac{-\Phi}{2Dt} + \frac{x^2\Phi}{4D^2t^2}\,.$$

into the diffusion equation (3.33).

Diffusive Transport As a function of the coordinate x, the solution (3.35) of the diffusion equation corresponds to a Gaussian with variance $\sigma^2 = 2Dt$. One hence concludes that the variance of the displacement follows diffusive behavior, i.e.

$$\langle x^2(t)\rangle = 2D\,t, \qquad \bar{x} = \sqrt{\langle x^2(t)\rangle} = \sqrt{2D\,t}\,, \tag{3.36}$$

where we assumed that the mean $\langle x\rangle = 0$ vanishes. Diffusive transport is therefore characterized by transport sublinear in time, in contrast to ballistic transport following $x = vt$. Compare Fig. 3.11.

Green's Function for Diffusion For general initial distributions $p_0(x) = p(x,0)$ of walkers the diffusion equation (3.33) is solved by

$$p(x,t) = \int dy\, \Phi(x-y,t)\, p_0(y)\,, \tag{3.37}$$

[8] Note that $\int \mathrm{e}^{-x^2/a}\mathrm{d}x = \sqrt{a\pi}$, together with $\lim_{a\to 0} \exp(-x^2/a)/\sqrt{a\pi} = \delta(x)$.

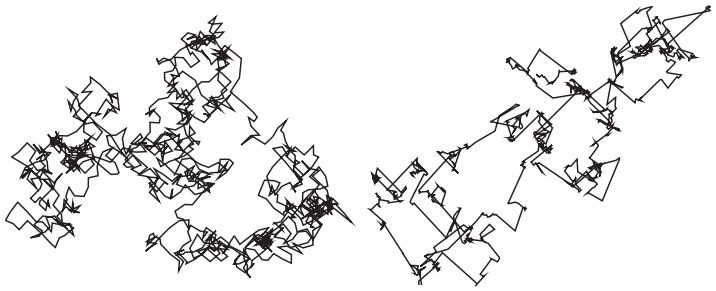

Fig. 3.11 Examples of random walkers with scale-free distributions $\sim 1/|\Delta x|^{1+\beta}$ for real-space jumps, see (3.39). **Left:** $\beta = 3$, which falls into the universality class of standard Brownian motion. **Right:** $\beta = 0.5$, a typical Levy flight. Note the occurrence of longer-ranged jumps in conjunction with local walking.

since $\lim_{t\to 0} \Phi(x-y,t) = \delta(x-y)$. An integral kernel allowing to construct the solution of a differential equation for arbitrary initial conditions is a "Green's function".

First Passage Time When starting from the origin, which is the typical time t_y a random walker would need to reach a certain distance $y > 0$ for the first time? We define the survival probability

$$S_y(t) = \int_{-\infty}^{y} dx \left[\Phi(x,t) - \Phi(x-2y,t)\right], \qquad S_y(0) = 1, \qquad S_y(\infty) = 0\,,$$

which denotes the probability that the walker is below y at time t, without having ever crossed the 'cliff' $x = y$. Here we used the solution (3.35) of the diffusion equation, as describing walkers starting respectively at $x = 0$ and $x = 2y$. Importantly, the kernel $\Phi(x,t) - \Phi(x-2y,t)$ vanishes for $x = y$. The survival probability is monotonically decreasing with increasing time. The first passage time $t = t_F$ is not fixed, but distributed as

$$F_y(t) = -\frac{d}{dt} S_y(t) = -D \int_{-\infty}^{y} dx \, \frac{d^2}{d^2x} \left[\Phi(x,t) - \Phi(x-2y,t)\right],$$

where we used the diffusion equation $\dot{\Phi} = D\Delta\Phi$ in one dimension below the integral. Direct integration yields

$$\begin{aligned} F_y(t) &= \frac{-D}{\sqrt{4\pi Dt}} \int_{-\infty}^{y} dx \, \frac{d^2}{dx^2} \left[\mathrm{e}^{-x^2/(4Dt)} - \mathrm{e}^{-(x-2y)^2/(4Dt)}\right] \\ &= \frac{-D}{\sqrt{4\pi Dt}} \frac{d}{dx} \left[\mathrm{e}^{-x^2/(4Dt)} - \mathrm{e}^{-(x-2y)^2/(4Dt)}\right]_{x=y} \\ &= \frac{y}{\sqrt{4\pi Dt^3}} \exp\left(-\frac{y^2}{4Dt}\right), \end{aligned} \tag{3.38}$$

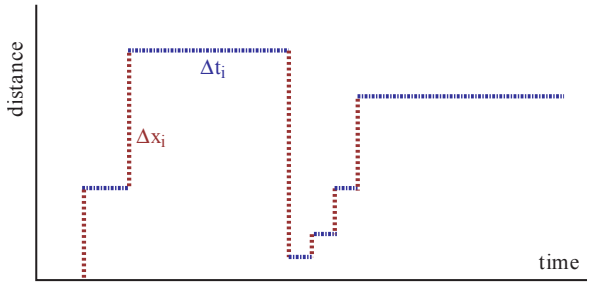

Fig. 3.12 A random walker with distributed waiting times Δt_i and jumps Δx_i may become a generalized Lévy flight, compare (3.39).

which is a "Lévy distribution".[9]

For fixed y, one has that (3.38) scales as $\sim t^{-\alpha}$ for large t, with $\alpha = 3/2$. The first moment of the first passage time density $F_y(t)$ diverges consequently.[10] An average first passage time is not defined.

Lévy Flights One can generalize the concept of a random walker, which is at the basis of ordinary diffusion, and consider a random walk with distributions $\rho(\Delta t)$ and $\rho(\Delta x)$ for waiting times Δt_i and jumps Δx_i, at time step $i = 1, 2, \ldots$ of the walk, as illustrated in Fig. 3.12. One may assume scale-free distributions

$$\rho(\Delta t) \sim \frac{1}{(\Delta t)^{1+\alpha}}, \qquad \rho(\Delta x) \sim \frac{1}{(\Delta x)^{1+\beta}}, \qquad \alpha, \beta > 0\,. \tag{3.39}$$

If $\alpha > 1$ (finite mean waiting time) and $\beta > 2$ (finite variance), nothing special happens. In this case the central limiting theorem for well behaved distribution functions is valid for the spatial component and one obtains standard Brownian diffusion. Relaxing the above conditions one finds four regimes: normal Brownian diffusion, "Lévy flights", fractional Brownian motion, also denoted "subdiffusion" and generalized Lévy flights termed "ambivalent processes". Their respective scaling laws are listed in Table 3.1, with two examples being shown in Fig. 3.11.

Lévy flights occur for a wide range of processes, such as for the flight patterns of wandering albatrosses. Human travel habits seem to be characterized by a generalized Lévy flight with $\alpha, \beta \approx 0.6$.

3.3.2 Markov Chains

For many common stochastic processes $x_1 \to x_2 \to x_3 \to \ldots$ the probability to visit a state $x_{t+1} = y$ depends solely on the current state $x_t = x$.

MARKOV PROPERTY A stochastic process is "markovian" if it has no memory.

[9] The Lévy distribution $\sqrt{c/(2\pi)}\exp(-\frac{c}{2t})/t^{3/2}$ is normalized on the interval $t \in [0, \infty]$.

[10] The moments of powerlaw distributions are discussed in Sect. **??** of Chap. **??**, "**??**".

A memory would be present, on the other hand, if the transition rule $x_t \to x_{t+1}$ would be functionally dependent on earlier x_{t-1}, x_{t-2}, ... elements of the process.

Absorbing States The transition probabilities $p(x, y)$ to visit a state $x_{t+1} = y$, when being at $x_t = x$, are normalized,

$$1 = \sum_y p(x, y), \qquad p(x, y) \geq 0\,, \tag{3.40}$$

since one always arrives to some state $x_{t+1} = y$ when starting from a given $x_t = x$. A process may stay in place, which occurs with the probability $p(x, x)$. A state x^* is "absorbing" whenever

$$p(x^*, x^*) = 1, \qquad p(x^*, y) = 0, \qquad \forall y \neq x^*\,. \tag{3.41}$$

A stochastic process can be viewed as being terminated, or "extinct", when reaching an absorbing state. The extinction probability is then the probability to hit x^* when starting from a given state x_0. A famous example is the Galton-Watson process, which describes the extinction probabilities of family names.[11]

Master Equation We consider density distributions $\rho_t(x)$ of walkers, with each walker having the same transition probabilities $p(x, y)$. For discrete times $t = 0, 1, \ldots$, the evolution of the density of walkers is given by the "master equation"

$$\begin{aligned} \rho_{t+1}(y) &= \rho_t(y) + \textstyle\sum_x \left[\, \rho_t(x)p(x, y) - \rho_t(y)p(y, x) \,\right] \\ &= \rho_t(y) + \textstyle\sum_x \rho_t(x)p(x, y) - \rho_t(y) \\ &= \textstyle\sum_x \rho_t(x)p(x, y)\,, \end{aligned} \tag{3.42}$$

where we took into account that the number of walkers is conserved, namely that $\sum_y p(x, y) = 1$. Random walks and any other stochastic time series, are described by their defining master equations.

Stationarity A Markov process becomes stationary when the distribution of walkers does not change anymore with time, viz when

[11] The Galton-Watson process will be treated in Sect. **??** of Chap. **??**, "**??**".

Table 3.1 The four regimes of a generalized walker with distribution functions, Eq. (3.39), characterized by scalings $\sim(\Delta t)^{-1-\alpha}$ and $\sim(\Delta x)^{-1-\beta}$ for the waiting times Δt and jumps Δx, as depicted in Fig. 3.12.

$\alpha > 1$	$\beta > 2$	$\bar{x} \sim \sqrt{t}$	Ordinary diffusion
$\alpha > 1$	$0 < \beta < 2$	$\bar{x} \sim t^{1/\beta}$	Lévy flights
$0 < \alpha < 1$	$\beta > 2$	$\bar{x} \sim t^{\alpha/2}$	Subdiffusion
$0 < \alpha < 1$	$0 < \beta < 2$	$\bar{x} \sim t^{\alpha/\beta}$	Ambivalent processes

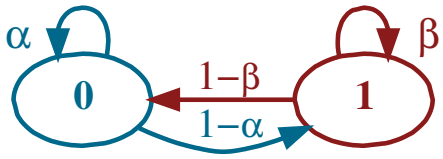

Fig. 3.13 The general two-state Markov chain, as defined by (3.43).

$$\rho^*(y) = \rho_{t+1}(y) = \rho_t(y), \qquad \sum_x \rho^*(x)p(x,y) = \rho^*(y), \qquad \rho^* P = \rho^* ,$$

where P is the transition matrix $p(x,y)$. The stationary distribution of walkers ρ^* is consequently a left eigenvector of P.

General Two-State Markov Process As an example we define with

$$P = \begin{pmatrix} \alpha & 1-\alpha \\ 1-\beta & \beta \end{pmatrix}, \qquad \alpha, \beta \in [0,1] \tag{3.43}$$

the transition matrix P for the general two-state Markov process, compare Fig. 3.13. The eigenvalues λ of the left eigenvectors $\rho^* = (\rho_1, \rho_2)$ of P are determined by

$$\begin{aligned} \alpha\,\rho_1 + (1-\beta)\rho_2 &= \lambda\rho_1 \\ (1-\alpha)\rho_1 + \beta\,\rho_2 &= \lambda\rho_2 \end{aligned} , \tag{3.44}$$

which has the solutions

$$\lambda_1 = 1, \qquad \rho^*_{\lambda_1} = \frac{1}{N_1}\begin{pmatrix} 1-\beta \\ 1-\alpha \end{pmatrix}, \qquad N_1 = \sqrt{(1-\alpha)^2 + (1-\beta)^2}$$

and

$$\lambda_2 = \alpha + \beta - 1, \qquad \rho^*_{\lambda_2} = \frac{1}{\sqrt{2}}\begin{pmatrix} 1 \\ -1 \end{pmatrix} .$$

The first eigenvalue dominates generically, $\lambda_1 = 1 > |\alpha + \beta - 1| = |\lambda_2|$, with the contribution to $\rho^*_{\lambda_2}$ dying out. Absorbing states are present whenever $\alpha/\beta = 1$, see Fig. 3.13.

Random Surfer Model A famous diffusion process is the "random surfer model" which tries to capture the behavior of Internet users. This model is at the basis of the original Page & Brin Google page-rank algorithm.

Consider a network of $i = 1, \ldots, N$ Internet hosts connected by directed hyperlinks characterized by the adjacency matrix A_{ij}.[12] We denote with

$$\rho_i(t), \qquad \sum_{i=1}^{N} \rho_i(t) = 1$$

[12] More about the adjaceny matrix in Sect. **??** of Chap. **??**, "**??**".

the probability of finding an Internet surfer visiting host i at time t. The surfers are assumed to perform a markovian walk on the Internet by clicking randomly any available out-going hyperlink, giving raise to the master equation

$$\rho_i(t+1) = \frac{c}{N} + (1-c)\sum_j \frac{A_{ij}}{\sum_l A_{lj}}\rho_j(t)\,. \tag{3.45}$$

Normalization is conserved,

$$\sum_i \rho_i(t+1) = c + (1-c)\sum_j \frac{\sum_i A_{ij}}{\sum_l A_{lj}}\rho_j(t) = c + (1-c)\sum_j \rho_j(t)\,.$$

Hence $\sum_i \rho_i(t+1) = 1$ whenever $\sum_j \rho_j(t) = 1$.

Google page rank The parameter c in the random surfer model regulates the probability to randomly enter the Internet:

- For $c = 1$ the adjacency matrix and hence the hyperlinks are irrelevant. We can interpret therefore c as the uniform probability to enter the Internet.
- For $c = 0$ a surfer never enters or leaves the Internet, continuing to click around forever, c is hence also the probability to stop clicking hyperlinks.

The random surfer model (3.45) can be solved iteratively. Convergence is fast for not too small c. At every iteration authority is transferred from one host j to other hosts i through its outgoing hyperlinks A_{ij}. The steady-state density ρ_i of surfers can hence be considered as a measure of host authority and is equivalent to the orginal Google page rank, which was an important score for ranking search results at the dawn of the Internet.

Relation to Graph Laplacian The continuous time version of the random surfer model can be derived, for the case $c = 0$, from

$$\frac{\rho_i(t+\Delta t) - \rho_i(t)}{\Delta t} = \sum_j \frac{A_{ij}}{k_j}\rho_j(t) \;-\; \rho_i(t), \qquad k_j = \sum_l A_{lj}\,,$$

where k_j is the out-degree of host j and Δt the time step. Taking the limit $\Delta t \to 0$ yields

$$\frac{d}{dt}\rho = \tilde{\Lambda}\,\rho, \qquad \tilde{\Lambda}_{ij} = -\frac{\Lambda_{ij}}{k_j}, \qquad \Lambda_{ij} = k_j\delta_{ij} - A_{ij}\,, \tag{3.46}$$

where Λ_{ij} is the Graph Laplacian.[13] Eq. (3.46) corresponds to a generalization of the diffusion equation (3.33) to networks.

[13] The Graph Laplacian is treated in Sect. **??** of Chap. **??**, "**??**".

3.4 Stochastic Systems

3.4.1 Langevin Equation

Diffusion as a Stochastic Process Langevin proposed to describe the diffusion of a particle by the stochastic differential equation,

$$m\,\dot{v} = -m\,\gamma\,v \,+\, \xi(t), \qquad \langle \xi(t) \rangle = 0, \qquad \langle \xi(t)\xi(t') \rangle = Q\delta(t-t')\,, \quad (3.47)$$

where $v(t)$ is the velocity of the particle and $m > 0$ its mass.

- The term $-m\gamma v$ on the right-hand-side of (3.47) corresponds to a damping term, the friction being proportional to $\gamma > 0$.
- $\xi(t)$ is a stochastic variable, viz noise. The brackets $\langle \ldots \rangle$ denote ensemble averages, i.e. averages over different noise realizations.
- As "white noise" (in contrast to "colored noise") one denotes noise with a flat power spectrum (as white light), viz $\langle \xi(t)\xi(t') \rangle \propto \delta(t-t')$.
- The constant Q is a measure for the strength of the noise.

All stochastic systems have a noise term on the right-hand side.

Solution of the Langevin Equation Considering a specific noise realization $\xi(t)$, one finds

$$v(t) = v_0\,\mathrm{e}^{-\gamma t} \,+\, \frac{\mathrm{e}^{-\gamma t}}{m} \int_0^t dt'\,\mathrm{e}^{\gamma t'}\,\xi(t') \quad (3.48)$$

for the formal solution of the Langevin equation (3.47), where $v_0 \equiv v(0)$.

Mean Velocity Taking the ensemble average $\langle v(t) \rangle$ of the velocity leads to

$$\langle v(t) \rangle = v_0\,\mathrm{e}^{-\gamma t} + \frac{\mathrm{e}^{-\gamma t}}{m} \int_0^t dt'\,\mathrm{e}^{\gamma t'}\,\underbrace{\langle \xi(t') \rangle}_{0} = v_0\,\mathrm{e}^{-\gamma t}\,. \quad (3.49)$$

The average velocity decays hence exponentially to zero.

Mean Square Velocity For the ensemble average $\langle v^2(t) \rangle$ of the velocity squared one finds

$$\begin{aligned} \langle v^2(t) \rangle \;\; &= \;\; v_0^2\,\mathrm{e}^{-2\gamma t} \,+\, \frac{2\,v_0\,\mathrm{e}^{-2\gamma t}}{m} \int_0^t dt'\,\mathrm{e}^{\gamma t'}\,\underbrace{\langle \xi(t') \rangle}_{0} \\ &\quad + \frac{\mathrm{e}^{-2\gamma t}}{m^2} \int_0^t dt' \int_0^t dt''\,\mathrm{e}^{\gamma t'}\,\mathrm{e}^{\gamma t''}\,\underbrace{\langle \xi(t')\xi(t'') \rangle}_{Q\,\delta(t'-t'')} \end{aligned}$$

$$= \; v_0^2\,\mathrm{e}^{-2\gamma t} \; + \; \frac{Q\,\mathrm{e}^{-2\gamma t}}{m^2} \underbrace{\int_0^t dt'\,\mathrm{e}^{2\gamma t'}}_{(\mathrm{e}^{2\gamma t}-1)/(2\gamma)} ,$$

and finally

$$\langle v^2(t)\rangle = v_0^2\,\mathrm{e}^{-2\gamma t} \; + \; \frac{Q}{2\,\gamma\,m^2}\,\left(1-\mathrm{e}^{-2\gamma t}\right) . \tag{3.50}$$

For long times the average squared velocity

$$\lim_{t\to\infty}\langle v^2(t)\rangle = \frac{Q}{2\,\gamma\,m^2} \tag{3.51}$$

becomes, as expected, independent of the initial velocity v_0. Eq. (3.51) shows explicitly that the dynamics is driven exclusively by the stochastic process $\propto Q$ for long time scales.

Langevin Equation and Diffusion The Langevin equation is formulated in terms of the particle velocity. In order to make connection with the time evolution of a real-space random walker, see (3.36), we multiply the Langevin equation by x, take at the same time the ensemble average,

$$\langle x\,\dot{v}\rangle = -\gamma\langle x\,v\rangle + \frac{1}{m}\langle x\,\xi\rangle . \tag{3.52}$$

We note that

$$x\,v = x\,\dot{x} = \frac{\mathrm{d}}{\mathrm{d}t}\frac{x^2}{2}, \qquad x\,\dot{v} = x\,\ddot{x} = \frac{\mathrm{d}^2}{\mathrm{d}t^2}\frac{x^2}{2} - \dot{x}^2$$

and

$$\langle x\xi\rangle = \left\langle \xi(t)\int_0^t v(t')dt'\right\rangle = \int_0^t dt'\int_0^{t'} dt''\frac{\mathrm{e}^{-\gamma(t'-t'')}}{m}\underbrace{\langle\xi(t)\xi(t'')\rangle}_{Q\delta(t-t'')} = 0\,,$$

where we have used (3.48) in the limit of large times and that $t'' < t$. We then find

$$\frac{\mathrm{d}^2}{\mathrm{d}t^2}\frac{\langle x^2\rangle}{2} - \langle v^2\rangle \;=\; -\gamma\,\frac{\mathrm{d}}{\mathrm{d}t}\frac{\langle x^2\rangle}{2}$$

for (3.52), or

$$\frac{\mathrm{d}^2}{\mathrm{d}t^2}\langle x^2\rangle \; + \; \gamma\,\frac{\mathrm{d}}{\mathrm{d}t}\langle x^2\rangle \;=\; 2\langle v^2\rangle \;=\; \frac{Q}{\gamma m^2}\,, \tag{3.53}$$

the latter with the help of the long-time result (3.51) for $\langle v^2\rangle$. The solution of (3.53) is

$$\langle x^2\rangle \;=\; \left[\gamma t - 1 + \mathrm{e}^{-\gamma t}\right]\,\frac{Q}{\gamma^3 m^2}\,. \tag{3.54}$$

For long times we find we

$$\lim_{t\to\infty}\langle x^2\rangle \simeq \frac{Q}{\gamma^2 m^2}\, t \equiv 2Dt, \qquad D = \frac{Q}{2\gamma^2 m^2} \tag{3.55}$$

that the solutions of the Langevin equation show diffusive behavior, compare (3.36). This result, that $D \propto Q$, underpins the notion that diffusion is microscopically due to a stochastic process.

Massless Limit We add an external force $F(x)$ to the Langevin equation (3.47),

$$\dot{x} = v, \qquad m\,\dot{v} = -m\,\gamma\,v + F(x) + \xi(t)\,, \tag{3.56}$$

where we included the definition $v = \dot{x}$ of the velocity. Keeping $\Gamma = m\gamma$ constant while taking the limit $m \to 0$ leads to a well defined diffusion constant $D = Q/(2\Gamma^2)$, as given by (3.55). In this limit, the Langevin equation reduces to

$$\Gamma\dot{x} = F(x) + \xi(t)\,. \tag{3.57}$$

For stochastic processes in non-physical settings, like in finance, one usually starts with (3.57), which may be further adapted to the problem at hand.

3.4.2 Stochastic Calculus

Stochastic effects may depend functionally on the location x, e.g. via

$$\Gamma\dot{x} = F(x) \,+\, b(x)\xi(t)\,, \tag{3.58}$$

which is called the "non-linear Langevin equation". While looking like a fairly innocuous term, $b(x)\xi$ is actually not uniquely defined. The random kicks the system receives at time t depend via $b(x) = b(x(t))$ on a yet undefined position $x(t)$. Eq. (3.58) needs hence to be supplemented with a rule on how to treat the last term. This is usually done by looking at an integral over a small time inveral $[t, t+\Delta t]$.

Ito Stochastic Calculus Assuming that the strength of the kicks received is determined by the position of the sytem immediately before the kick takes place is consistent with the substitution

$$\int_t^{t+\Delta t} dt'\, b(x(t'))\,\xi(t') \quad \to \quad b(x(t)) \int_t^{t+\Delta t} dt'\,\xi(t')\,, \tag{3.59}$$

which is known as the "Ito stochastic calculus".

Stratonovich Stochastic Calculus Alternatively, one may assume that the strength of the individual kicks depend on a suitable average of the position. A possibility to model this situation is to substitute

$\int_t^{t+\Delta t} dt'\, b(x(t'))\, \xi(t')$ by

$$\frac{b(x(t)) + b(x(t+\Delta t))}{2} \int_t^{t+\Delta t} dt'\, \xi(t')\,, \tag{3.60}$$

which is known as the "Stratonovich stochastic calculus". The two formalisms, Stratonovich and Ito, lead in general to different results. In physics, Stratonovich is usually the correct choice, with Ito describing what happens in finance.

3.5 Noise-Controlled Dynamics

Stochastic Systems A set of first-order differential equations with a stochastic term is generally denoted a "stochastic system". The Langevin equation (3.47) is a prominent example. Depending on the circumstances, the stochastic component may determine the long-term dynamical behavior alltogether. Some examples.

- Neural Networks
  Networks of interacting neurons are responsible for the cognitive information processing in the brain. They must remain functional also in the presence of noise and be stable as stochastic systems. In this case the introduction of a noise term to the evolution equation should not change the dynamics qualitatively. This postulate should be valid for the vast majorities of biological networks.
- Diffusion
  The Langevin equation reduces, in the absence of noise, to a damped motion without an external driving force, with $v = 0$ acting as a global attractor. The stochastic term is therefore essential in the long-time limit, leading to diffusive behavior, with $\langle x^2 \rangle \propto t$.
- Stochastic Escape and Stochastic Resonance
  A particle trapped in a local minimum may escape the minimum by a noise-induced diffusion process; a phenomenon denoted "stochastic escape". Stochastic escape in a driven bistable system leads to an even more subtle consequence of noise-induced dynamics, "stochastic resonance".

In the following we detail out both stochastic escape and stochastic resonance.

3.5.1 Fokker–Planck Equation

Drift Velocity We add an external potential $V(x)$ to the Langevin equation (3.47),

$$m\,\dot{v} = -m\,\gamma\,v + F(x) + \xi(t), \qquad F(x) = -V'(x) = -\frac{d}{dx}V(x)\,, \tag{3.61}$$

where v and m are the velocity and the mass of the particle, $\langle \xi(t) \rangle = 0$ and $\langle \xi(t)\xi(t') \rangle = Q\delta(t-t')$. In the absence of damping and noise, when $\gamma = 0 = Q$, Eq. (3.61) reduces to Newton's law.

We consider for a moment a constant force $F(x) = F$ and the absence of noise, $\xi(t) \equiv 0$. The system reaches an equilibrium for $t \to \infty$ when relaxation and force cancel each other:

$$m\,\dot{v}_D = -m\,\gamma\,v_D + F \equiv 0, \qquad v_D = \frac{F}{\gamma m}\,. \tag{3.62}$$

v_D is called the "drift velocity". A typical example is the motion of electrons in a metallic wire. As described by Ohm's law, an applied voltage leads to an electric field along the wire, which induces in turn an electrical current. As a result one has drifting electrons that are continuously accelerated by the electrical field, while bumping into lattice imperfections or colliding with the lattice vibrations, i.e. with phonons.

Continuity Equation Generalizing to an ensemble of particles diffusing in an external potential, we denote with $P(x,t)$ the density of particles at location x and time t. Particle number conservation defines the particle current density $J(x,t)$ via the continuity equation

$$\frac{\partial P(x,t)}{\partial t} + \frac{\partial J(x,t)}{\partial x} = 0. \tag{3.63}$$

There are two contributions, J_D and J_ξ, to the total particle current density, $J = J_D + J_\xi$, induced respectively by diffusion and by stochastic motion. We derive these two contributions in two steps.

Drift and Diffusion Currents In a first step we disregard noise in (3.61) and set $Q = 0$. In the stationary limit particles move in this case uniformly, with the drift velocity v_D. The respective current density is

$$J_D = v_D\,P(x,t)\,.$$

In a second step we derive the contribution J_ξ of the noise term $\sim \xi(t)$ to the particle current density by setting the force term to zero, $F = 0$. For this purpose we rewrite the diffusion equation (3.33) with

$$\frac{\partial P(x,t)}{\partial t} = D\,\frac{\partial^2 P(x,t)}{\partial x^2} \equiv -\frac{\partial J_\xi(x,t)}{\partial x} \qquad \frac{\partial P(x,t)}{\partial t} + \frac{\partial J_\xi(x,t)}{\partial x} = 0$$

as a continuity equation, which allows us to determine the functional form of J_ξ,

$$J_\xi = -D\frac{\partial P(x,t)}{\partial x}\,. \tag{3.64}$$

Fokker–Planck Equation We recall the relation $D = Q/(2\gamma^2 m^2)$ between the diffusion constant D and the amplitude of the noise term Q, see (3.55). Adding both current contributions, we obtain

$$\begin{aligned} J(x,t) &= v_D\, P(x,t) - D\,\frac{\partial P(x,t)}{\partial x} \\ &= \frac{F}{\gamma m}\, P(x,t) - \frac{Q}{2\gamma^2 m^2}\,\frac{\partial P(x,t)}{\partial x} \end{aligned} \tag{3.65}$$

for the total current density $J = J_D + J_\xi$. Substituting this expression for the total particle current density into the continuity equation, see (3.63), one obtains the "Fokker–Planck" or "Smoluchowski" equation

$$\frac{\partial P(x,t)}{\partial t} = -\frac{\partial v_D\, P(x,t)}{\partial x} + \frac{\partial^2 D\, P(x,t)}{\partial x^2}\,, \tag{3.66}$$

aka the master equation of the density distribution $P(x,t)$. The first and second term on the right-hand side correspond respectively to ballistic and diffusive transport. Without going into details, we note that above expression for the Fokker–Planck equation is consistent with the Ito stochastic calculus, as defined by (3.59).

3.5.2 Stochastic Escape

Harmonic Potential One can solve the Fokker–Planck equation (3.66) analytically for a harmonic confining potential,

$$V(x) = \frac{f}{2}\,x^2, \qquad F(x) = -f\,x\,.$$

We are interested in particular in the stationary density distribution,

$$\frac{dP(x,t)}{dt} = 0 \qquad \Longrightarrow \qquad \frac{dJ(x,t)}{dx} = 0\,,$$

where the second equation follows from the continuity condition (3.63). With (3.65) for the total current density we find

$$\frac{d}{dx}\left[\frac{f\,x}{\gamma\,m} + \frac{Q}{2\gamma^2 m^2}\frac{d}{dx}\right] P(x) = 0 = \frac{d}{dx}\left[\beta f x + \frac{d}{dx}\right] P(x)\,,$$

where we used $F = -fx$ in (3.65). We defined $\beta = 2\gamma m/Q$ together with the stationary limit $P(x) = \lim_{t\to\infty} P(x,t)$ for the distribution of random walkers. The system is confined, which implies that the steady-state current vanishes, which implies in turn that

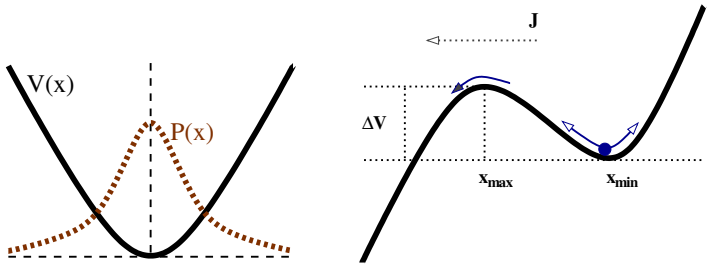

Fig. 3.14 Left: Stationary distribution $P(x)$ of diffusing particles in a harmonic potential $V(x)$. **Right:** Stochastic escape from a local minimum, with $\Delta V = V(x_{\max}) - V(x_{\min})$ being the potential barrier height and J the escape current.

$$0 = \left[\beta f x + \frac{d}{dx}\right] P(x) \tag{3.67}$$

holds. The corresponding solution is

$$P(x) = A\,\mathrm{e}^{-\beta f x^2/2} = A\,\mathrm{e}^{-\beta V(x)}, \qquad A = \frac{1}{\sqrt{2\pi\sigma^2}}\,, \tag{3.68}$$

where $\sigma^2 = 1/(\beta f) = Q/(2f\gamma m)$, with normalization condition $\int dx P(x) = 1$ being fulfilled. The density of diffusing particles in a harmonic trap is Gaussian-distributed, see Fig. 3.14.

Escape Current We now consider particles in a local minimum, as depicted in Fig. 3.14. A typical partially confining potential has a functional form like

$$V(x) \;\sim\; -x \,+\, x^3\,. \tag{3.69}$$

Without noise, the particle will oscillate around the local minimum eventually coming to a standstill under the influence of friction, with $x \to x_{\min}$. With noise, the particle will have a small but finite probability

$$\propto \mathrm{e}^{-\beta\Delta V}, \qquad \Delta V = V(x_{\max}) - V(x_{\min})$$

to reach the next saddle, where ΔV is the potential difference between the saddle and the local minimum, see Fig. 3.14.

The solution (3.68) for the stationary particle distribution in a confining potential $V(x)$ has a vanishing total current J. For non-confining potentials, like (3.69), the particle current $J(x,t)$ never vanishes. Stochastic escape occurs when starting with a density of diffusing particles close the local minimum, as illustrated in Fig. 3.14. The escape current will be nearly constant whenever the escape probability is small. In this case the escape current

$$J(x,t)\Big|_{x=x_{\max}} \;\propto\; \mathrm{e}^{-\beta\,[V(x_{\max})-V(x_{\min})]}\,,$$

will be proportional to the probability a particle has to reach the saddle. Functionally, we did approximate $P(x)$ with one valid for a perfect harmonic potential, as given by (3.68).

Kramer's Escape When the escape current is finite, there is a finite probability per unit of time for the particle to escape the local minima, the "Kramer's escape rate", r_K,

$$r_K = \frac{\omega_{\max}\omega_{\min}}{2\pi\,\gamma}\,\exp\left[-\beta\,(V(x_{\max}) - V(x_{\min}))\right], \tag{3.70}$$

where $\beta = 2\gamma m/Q$ and where the prefactors can be derived from a more detailed calculation, with $\omega_{\min}^2 = |V''(x_{\min})|/m$ and $\omega_{\max}^2 = |V''(x_{\max})|/m$.

Stochastic Escape in Evolution Stochastic escape occurs in many real-world systems. Noise allows the system to escape from a local minimum where it would otherwise remain stuck for eternity. As an example, we mention stochastic escape from a local fitness maximum (in evolution fitness is to be maximized) by random mutations that play the role of noise.[14]

3.5.3 Stochastic Resonance

Driven Double-Well Potential We consider diffusive dynamics in a driven double-well potential, see Fig. 3.15,

$$\dot{x} = -V'(x) + A_0\cos(\Omega t) + \xi(t), \qquad V(x) = -\frac{1}{2}x^2 + \frac{1}{4}x^4\,. \tag{3.71}$$

Several remarks.

- Eq. (3.71) is an example for a Langevin equation in the massless limit (3.57), here with $\Gamma = m\gamma = 1$. Friction has hence been taken to diverge.
- For the potential $V(x)$ a normal form has been taken, which one can always achieve by rescaling variables appropriately.
- The potential has two stable minima x_0,

$$-V'(x) = 0 = x - x^3 = x(1-x^2), \qquad x_0 = \pm 1\,.$$

  The local maximum at $x_0 = 0$ is unstable.
- We assume that the periodic driving $\propto A_0$ is small enough, such that the effective potential $V(x) - A_0\cos(\Omega t)x$ retains two minima at all times, compare Fig. 3.15.

Transient State Dynamics The system will stay close to one of the two minima, $x \approx \pm 1$, for most of the time when both A_0 and the noise strength

[14] Stochastic escape from local fitness maxima will be discussed in more detail in Sect. ?? of Chap. ??, "??".

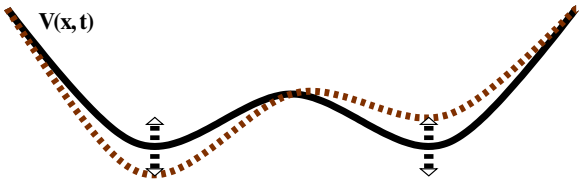

Fig. 3.15 The driven double-well potential, $V(x) - A_0 \cos(\Omega t)x$, compare (3.71). The driving force is small enough to retain the two local minima.

are weak, as illustrated in Fig. 3.16. The dynamics is therefore characterized by rapid transitions between transiently stable states.

Switching Times An important question is then: How often does the system switch between the two preferred states $x \approx 1$ and $x \approx -1$? There are two time scales present.

– Stochastic Escape
  In the absence of external driving, $A_0 \equiv 0$, the transitions are noise driven and irregular, with the average switching time given by Kramer's lifetime $T_K = 1/r_K$, see Fig. 3.16. The system is translational invariant with respect to time and the ensemble averaged expectation value

$$\langle x(t) \rangle \;=\; 0$$

  therefore vanishes in the absence of an external force.
– External Forcing
  When $A_0 \neq 0$ the external force induces a reference time together with a non-zero response $\bar{x}$,

$$\langle x(t) \rangle = \bar{x} \, \cos(\Omega t - \bar{\phi}) \,, \tag{3.72}$$

  which follows the time evolution of the driving potential with a certain phase shift $\bar{\phi}$, see Fig. 3.17.

The phenomenon of stochastic resonance regards the size of the response, as measured by $\bar{x}$

Resonance Condition When the time scale $2T_K = 2/r_K$ to switch back and forth due to the stochastic process equals the period $2\pi/\Omega$, we expect a large response $\bar{x}$, see Fig. 3.17. The time-scale matching condition

$$\frac{2\pi}{\Omega} \;\approx\; \frac{2}{r_K}$$

depends via (3.70) on the noise-level Q, which enters the Kramer's escape rate r_K. For otherwise constant parameters, the response $\bar{x}$ first increases with rising Q, decreasing however for elevated noise levels Q. This is the telltale characteristic of "stochastic resonance", as shown in Fig. 3.17.

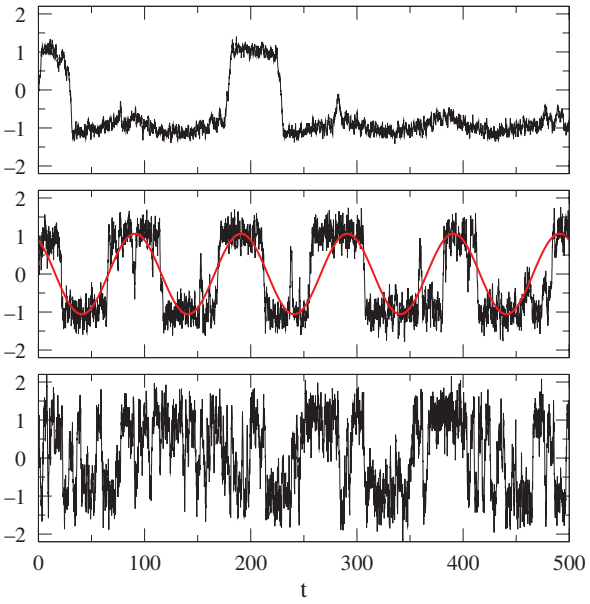

Fig. 3.16 Example trajectories $x(t)$ for the driven double-well potential. The strength and the period of the driving potential are $A_0 = 0.3$ and $2\pi/\Omega = 100$, respectively. The noise level Q is 0.05, 0.3 and 0.8 (top/middle/bottom), see (3.71).

Ice Ages The average temperature T_e of the earth differs by about $\Delta T_e \approx 10\,^\circ\mathrm{C}$ in between a typical ice age and interglacial periods. Both states of the climate are locally stable.

- Ice Age
  A substantial ice covering increases the albedo of the earth, which leads in turn to a larger part of sunlight to be reflected back to space. Earth remains cool.
- Interglacial Period
  The ice covering is reduced. A larger portion of the sunlight is absorbed by the oceans and land, with earth remaining warm.

A parameter of the orbit of planet earth, the eccentricity, varies slightly with a period $T = 2\pi/\Omega \approx 10^5$ years. The intensity of the incoming radiation from the sun therefore varies with the same period. Long-term climate changes can therefore be modeled by a driven two-state system, i.e. by (3.71). The driving force, viz the variation of the energy flux the earth receives from the sun, is however small. The increase in the amount of incident sunlight is too weak to pull the earth out of an ice age into an interglacial period or vice versa. Random climatic fluctuation, like variations in the strength of ocean circulations, are needed to finish the job. The alternation of ice ages with interglacial periods may therefore be modeled as a stochastic resonance phenomenon.

Beyond Stochastic Resonance Resonance phenomena generally occur when two frequencies, or two time scales, match as a function of some control

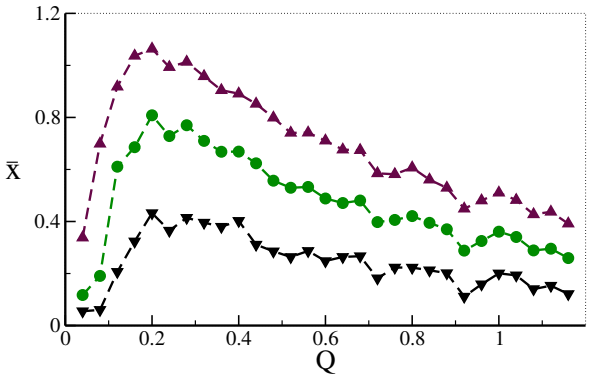

Fig. 3.17 The gain $\bar{x}$, see (3.72), as a function of noise level Q. The strength of the driving amplitude A_0 is 0.1, 0.2 and 0.3 (bottom/middle/top curves), see (3.71) and the period $2\pi/\Omega = 100$. The response $\bar{x}$ is very small for vanishing noise $Q = 0$, when the system performs only small-amplitude oscillations in one of the local minima.

parameter. For the case of stochastic resonance these two time scales correspond to the period of the external driving and to the average waiting time for Kramer's escape respectively, with the latter depending directly on the level of the noise. The phenomenon is denoted as stochastic resonance since one of the time scales involved is controlled by noise.

One generalization of stochastic resonance is "coherence resonance". In this case one has a dynamical system with two internal time scales, say t_1 and t_2. These two time scales can be affected to a different degree by an additional source of noise. An additional stochastic term may therefore change the ratio t_1/t_2, leading to internal resonance phenomena.